

TIME-VARIANT GRAY-BOX MODELING OF A PHASER PEDAL

Roope Kiiski, Fabián Esqueda* and Vesa Välimäki

Aalto University
 Department of Signal Processing and Acoustics
 Espoo, Finland
 roope.kiiski@aalto.fi

ABSTRACT

A method to measure the response of a linear time-variant (LTV) audio system is presented. The proposed method uses a series of short chirps generated as the impulse response of several cascaded allpass filters. This test signal can measure the characteristics of an LTV system as a function of time. Results obtained from testing of this method on a guitar phaser pedal are presented. A proof of concept gray-box model of the measured system is produced based on partial knowledge about the internal structure of the pedal and on the spectral analysis of the measured responses. The temporal behavior of the digital model is shown to be very similar to that of the measured device. This demonstrates that it is possible to measure LTV analog audio systems and produce approximate virtual analog models based on these results.

1. INTRODUCTION

Historically, guitar effect pedals have been designed and implemented using analog circuitry. Nowadays, digital effects have become more common and widely accepted, as they are more versatile and their costs can be reduced. Yet many of the old, analog devices have cult-like following, due to their alleged distinctive sound or their association with famous musicians [1]. Vintage analog pedals are rare and can reach high prices in secondary markets [2]. Therefore, to cater to consumers who are after particular effects, virtual analog modeling of these classic devices is needed. Some research on modeling different distortion, fuzz, reverb, and delay units can be found in literature [1, 3]. One particular effect, the *phaser*, is an interesting topic of study due to its time-varying nature. In this paper, an overview on the internal workings of a phaser is given. Then, a method to measure time-varying linear effects is introduced, along with results obtained from measuring a phaser pedal. These results are then used to develop a digital model of the phaser effect.

Two opposite system modeling approaches are ‘black-box’ and ‘white-box’ models [1]. Black-box models are such that the modeling is entirely based on input-output measurements of the system and there is no knowledge of the inner workings of the system. An example of black-box modeling of effect units can be found in [4]. On the other hand, white-box models are based on circuit analysis or other form of knowledge of how the system works. A white-box model of a phaser pedal was presented by Eichas et al. [2]. The technique followed in this study falls under the category of ‘gray-box’ modeling, which is defined as an approach where some knowledge of the internal characteristics of the system is used when modeling it based on measurements [1].

This paper is organized as follows. Section 2 discusses phasing using allpass filters. In Section 3, the steps necessary to measure the time-varying response of a phaser are presented. Section 4 presents the measured responses of an analog phaser pedal. Section 5 shows how the measured response is modeled in the digital domain. Finally, concluding remarks are given in Section 6.

2. BASICS OF PHASING

The phasing effect introduces time-varying notches in the spectrum of the input signal, creating a characteristic *swooshing* sound. Historically-famous phaser pedals, such as the MXR series and the Uni-Vibe, work by feeding a copy of the input signal into a chain of identical first-order allpass filters and mixing the output of this chain with the original signal [2, 3]. In this design, the location of the notches is determined by the break frequencies of the filters, which are modulated by a low frequency oscillator (LFO).

The block diagram for a basic digital phaser is shown in Fig. 1. By adjusting the *wetness* of the phaser, i.e. the ratio between original and filtered signals, using gain parameters G and W , the depth of the notches and the overall intensity of the effect can be controlled. To keep the output signal bounded, G and W are usually coupled so that $G = 1 - W$. The deepest possible notches are obtained when $W = G$. In this architecture, the number of notches introduced is determined by the number of the first-order allpass filters used, so that for N allpass filters (assuming N is even), $N/2$ notches are produced on positive frequencies. Usually the number of allpass filters in phasers is even.

The transfer function of a first-order digital allpass filter is

$$A(z) = \frac{a_1 + z^{-1}}{1 + a_1 z^{-1}}, \quad (1)$$

where coefficient a_1 , which also determines the pole, is defined in

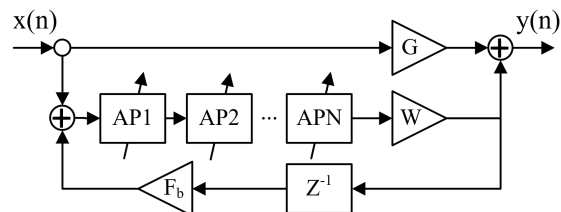


Figure 1: Block diagram of a digital phaser with a feedback loop via a unit delay. In most common phasers, there is no feedback loop, meaning that their $F_b = 0$.

* The work of F. Esqueda is funded by the Aalto ELEC Doctoral School.

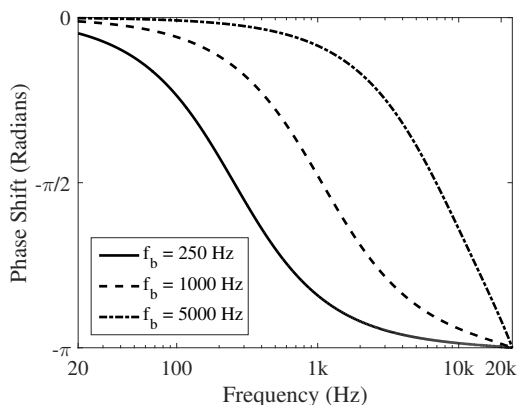


Figure 2: Phase response of a first-order allpass filter with break frequencies 250 Hz ($a_1 = -0.967$), 1000 Hz ($a_1 = -0.869$), and 5000 Hz ($a_1 = -0.346$).

terms of ω_b , the break frequency of the filter in rad/s, as

$$a_1 = -\frac{1 - \tan(\omega_b T/2)}{1 + \tan(\omega_b T/2)} \approx -\frac{1 - \omega_b T/2}{1 + \omega_b T/2} \approx -1 + \omega_b T, \quad (2)$$

where T is the sampling period of the system. For stability, the condition $|a_1| < 1$ is required [5]. The phase response of the allpass filter (1) as a function of angular frequency ω is given by

$$\Theta(\omega) = -\omega + 2 \arctan\left(\frac{a_1 \sin \omega}{1 + a_1 \cos \omega}\right). \quad (3)$$

During phasing, the allpass filter chain itself does not change the magnitude spectrum of the signal; it causes *phase shifting* [6]. From (3), we observe that each first-order allpass filter causes a frequency shift of $-\pi$ radians at half the sampling frequency (i.e. at $\omega = \pi$). At the break frequency the filter will introduce a phase shift of exactly $-\pi/2$ rad/s [7, 8]. Fig. 2 shows example phase responses of the first-order allpass filter with three different break frequencies. The sample rate $f_s = 1/T$ in these and all other examples in this paper is 44.1 kHz.

When several allpass filters are cascaded, their combined phase response is the sum of the individual phase responses. So, when N first-order allpass filters are cascaded, their combined phase response will introduce a maximum phase shift of $-N\pi$ radians. In this case, we assume N to be a positive even integer. Adding the filtered and original signals will cause notches at the frequencies at which the phase shift is an exact odd integer multiple of $-\pi$ rad/s, or $-k\pi$ with $k = 1, 3, 5, \dots, N - 1$ [3, 6, 7, 9]. Fig. 3 shows the phase response of two, four, and six cascaded allpass filters, highlighting the frequencies where notches will appear in a phasing scenario.

The position of the spectral notches in a phaser is changed over time by modulating the break frequencies of the filters using an LFO. The LFO usually has a frequency in the range from 0.1 to 10 Hz, and its waveform is typically triangular or sinusoidal. In analog phasers, the LFO changes the physical values of components in the allpass filters. In digital implementations, the LFO controls the coefficients of the allpass filters [3, 6, 8].

A limitation of using first-order allpass filters to implement phasers is that the width of the notches cannot be modified independently. Both the notch width and depth are controlled using

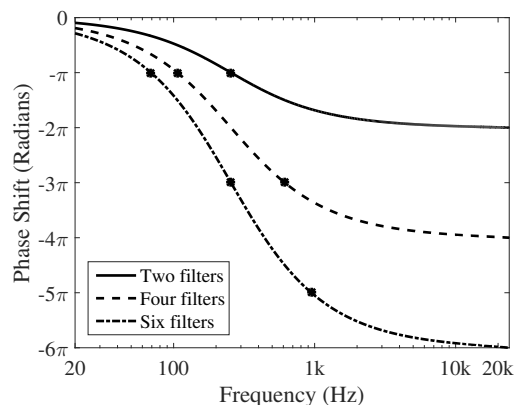


Figure 3: Phase response of two, four, and six cascaded first-order allpass filters with break frequency at 250 Hz ($a_1 = -0.967$). The squares indicate the resulting notch frequencies in each case, when used in a phaser.

the wetness parameter W , which changes both of them simultaneously. Additionally, controlling the location of the notches is not trivial. Both of these issues can be addressed by using second-order allpass filters instead, as they allow a more independent control of the notch characteristics [9].

Instead of using allpass filters, phasers can also be implemented by using cascaded notch filters [3, 10]. Notch filters allow better control of notch locations and depth than allpass filters. However, phasers implemented in this manner are more complex and expensive than their allpass counterparts [3, 10]. In analog phasers, more complexity means more physical components, higher costs, and bigger pedals. On the other hand, in a digital implementation the complexity may not represent such a big problem, but should still be considered [3].

Some phasers incorporate a feedback loop in their structure, feeding the output of the allpass chain back into its input. This architecture is illustrated in Fig. 1. A unit delay was inserted to this feedback path to avoid having a delay-free loop [8]. The summing of the output of the allpass chain with the input signal causes a similar effect as the summing of the output with the original signal, as again the two added signals have the phase difference of $-\pi$, -3π , -5π , etc. at certain frequencies. In practice, the feedback loop causes drastic changes in the magnitude response of the phaser, since resonances are introduced and the frequencies between the notches are boosted. This changes the overall shape of the magnitude response, as shown in Fig. 4 [7, 8].

3. MEASURING A TIME-VARIANT SYSTEM

Linear time-invariant (LTI) systems are typically analyzed by measuring their impulse response using a sine sweep, white noise, or another test signal of long duration. The time-varying nature of phasers means that these methods are unreliable, as the response of the system changes over time. To counter this, the measurement signal used must be short and should be played repeatedly through the system in order to observe the response of the system at different moments in time.

In this work, we assume the system under study to be linear and time-variant (LTV), i.e. it varies over time but does not intro-

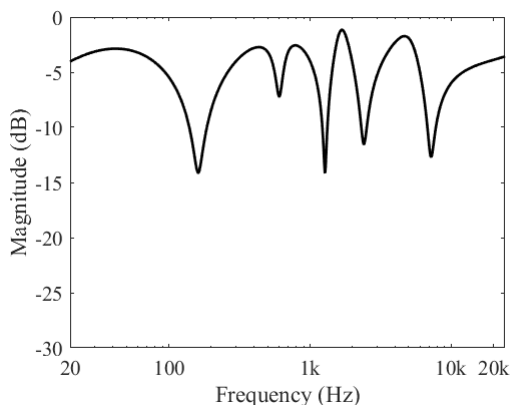


Figure 4: Magnitude response of a phaser having ten first-order allpass filters and a feedback loop ($F_b = 0.4$, $G = 0.5$, $W = 0.5$). Four of the allpass filters use the coefficient value -0.9490 and six use -0.8991 .

duce harmonic distortion. This condition is mostly true for filter-based non-saturating effects, such as the phaser, when the input signal level is not very high. The following subsections describe the measurement process used to evaluate the frequency response of an LTV system.

3.1. Measurement signal

To measure the response of an LTV system at an arbitrary moment in time, we must first design a short test signal. This signal should be short enough to guarantee the system being measured will remain fairly static during the measurement process. Arnardottir et al. used an impulse train to measure the behavior of a time-varying tape delay effect [11]. Alternatively, a very short chirp can be used for this purpose, since it yields an improved signal-to-noise ratio (SNR). Such a signal is described in [5] and [12]. Repeatedly evaluating the instantaneous response of the system over a period of time will allow us to observe its time-varying response.

Following the work of [5] and [12], we can synthesize a chirp using the impulse response of a cascade of first-order allpass filters. The idea is that even though allpass filters do not alter the frequency content of a signal, when dozens of them are cascaded, the result is a system that introduces significantly different delays for different frequencies. These differences cause frequencies to be played at different times, similar to a sine sweep. The advantage of synthesizing a chirp in this manner is that extremely short signals, e.g. 10 or 50 ms long, can be produced with relative ease [5, 12]. In sine sweep measurements, the minimum length of the signal is limited by the low frequencies [12]. The lower the frequencies that need to be measured, the longer the sine sweep must be.

As indicated by (3), the pole a_1 of the first-order allpass filter determines the overall phase response of the filter. Since the phase-shift and group delay are closely related, this pole also changes the group delay of the filter. The group delay of a single first-order allpass filter can be calculated with the following formula:

$$\tau_g(\omega) = \frac{1 - a_1^2}{1 + 2a_1 \cos(\omega) + a_1^2}, \quad (4)$$

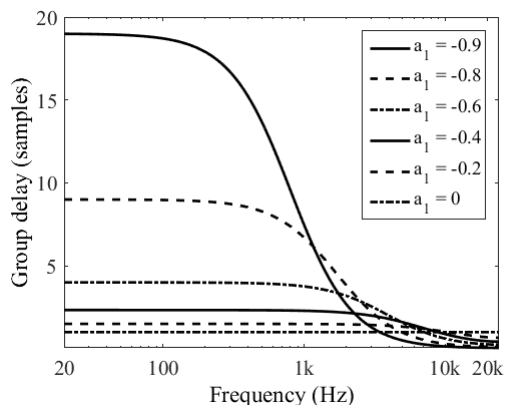


Figure 5: Group delay of a first-order digital allpass filter with different coefficient values.

where ω is angular frequency. Fig. 5 illustrates the group delay of a first-order allpass filter for different poles values. As can be noted, the group delays are very small even for large pole values, less than 20 samples. However, when several allpass filters are cascaded, their group delays are added, so with ten filters in cascade the total group delay at low frequencies is almost 200 samples [5].

The group delay curves show that the resulting chirp-like impulse response first plays the high frequencies and then sweeps downwards to the lowest frequency. A chirp constructed using 64 allpass filters by setting $a_1 = -0.9$ is shown in Fig. 6. We can see that the chirp is only about 1500 samples long (approx. 30 ms), yet it still covers all the frequencies of interest [5].

In addition to meeting the requirement of being short, this chirp can be easily repeated periodically, which makes it a suitable test signal for LTV devices. Additionally, the way in which this signal is generated has one significant advantage; since the chirp is generated by feeding an impulse into an allpass filter chain, this impulse can be reconstructed by processing the chirp backwards through the same filter chain. In fact, this operation implements the deconvolution, which is needed to retrieve the impulse response of a system. This makes measuring LTV systems with a signal containing multiple chirps simple, as the measured signal can then be processed backwards through the allpass filter chain. The resulting multiple responses can be analyzed, generating a picture of how the magnitude response of the system changes over time [12].

The fact that the unprocessed chirp can be reverted back into an impulse means that several chirps can be superimposed (added) within a short time period. In fact, they may overlap in time. The only restriction for the spacing of the chirps is that when the signal is reverted back through the allpass chain, the resulting impulse responses should not overlap. If they do, the analysis cannot be performed so easily. A measurement signal with a duration of approx. 1 s, synthesized using chirps generated by 64 allpass filters with coefficient $a_1 = -0.9$ (see Fig. 6), spaced at 30 ms intervals is shown in Fig. 7. This figure illustrates the test signal in the time domain, containing a total of 33 chirps in 1 s.

3.2. Measurement analysis

The aim of this work is to measure a real phaser pedal and observe all the interesting aspects about its behavior. For a basic phaser

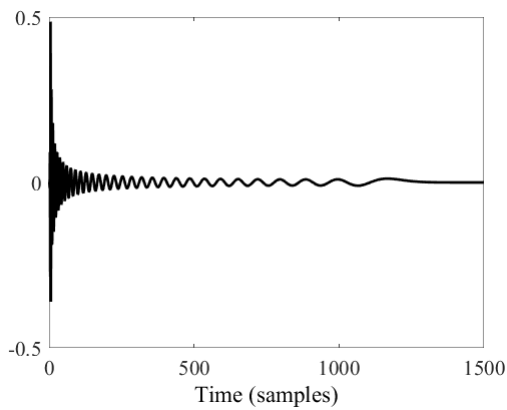


Figure 6: Time-domain waveform of a single chirp synthesized using 64 first-order allpass filters with pole parameter $a_1 = -0.9$.

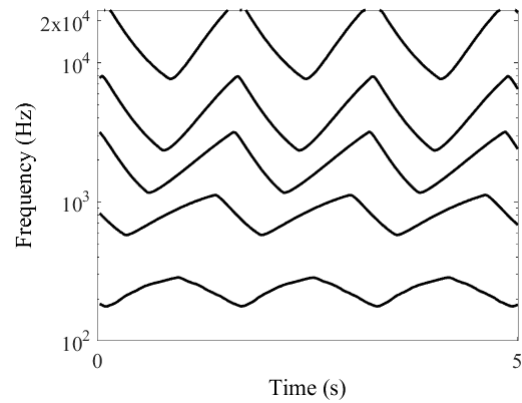


Figure 8: Distorted minima locations measured with a chirp generated with 2,048 allpass filters, which is too long.

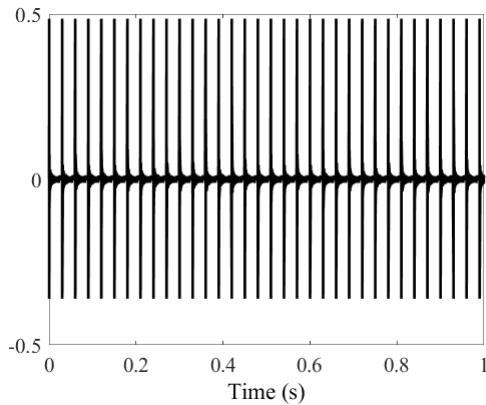


Figure 7: Time-domain waveform of an example measurement signal synthesized using 33 overlapping chirps (see Fig. 6).

pedal with only a speed knob, this can be achieved by measuring the pedal at different speed settings. From the obtained measurements we wish to observe the behavior and shape of the LFO, along with the number and position of the notches over time.

The notches caused by a phaser can be identified by finding the minima of the magnitude responses. To do so, the following procedure was followed. First, the global minimum of the magnitude spectrum was found. Once the location of the global minimum was known, the adjacent local maxima were found, and the area between these two local maxima was zeroed out. After the original global minimum of the spectrum was removed, the next one was found by repeating these steps. This process was repeated until all the minima were found.

In this study, when converting the magnitude values to dB-scale, a reference value of 1.7325 was used. This is the maximum value of the spectrum of the first chirp used on the first measurement. This value was chosen so that for all measurements, spectra, and other values can easily be compared with each other.

An interesting aspect about the proposed measurement method is how it reacts to changes in the length of the chirps forming the measurement signal. If the chirps are too long, the minima will appear to be ‘out of sync’. Due to the nature of the chirp, high

frequencies are played before low frequencies. When high frequencies are processed, the minima will be at a given location; later, when the low frequencies pass through the system, the minima locations will have already moved. This was tested by playing signals with different chirp lengths through a phaser pedal and observing how the resulting data changed. The chirp length was adjusted by increasing the amount of cascaded allpass filters used to generate it. The chirp was generated with 2,048 allpass filters in cascade, with coefficient $a_1 = -0.9$, which resulted in a chirp that is roughly 40,000 samples long. The total test signal lasted for 240,000 samples, with the chirps overlapping. The measured results are shown in Fig. 8, where it can be clearly observed that the minima do not occur at the same time. This can be corrected by using shorter chirps. With these tests it was also noticed that increasing the chirp length increases the SNR of the measured signal.

As expected, when the chirp length is very short, the SNR of the measurement becomes low and the measured magnitude spectrum has clear artefacts. Therefore, it is desirable to find an optimal chirp length with which the spectral minima appear to be synchronized at the same time with a good SNR. In this work, the measurements were conducted with a chirp generated using a cascade of 64 first-order allpass filters with $a_1 = -0.9$, which was repeated every 0.03 s.

4. MEASUREMENT RESULTS

The phaser pedal chosen for this study is the Fame Sweet Tone Phaser PH-10. The similarities between the general appearance of this pedal and the MXR Phase 100 suggest that the measured pedal is a clone of the Phase 100.

The measured pedal has a single ‘speed’ potentiometer and two switches. These switches are grouped and labeled simply as ‘Intensity’. Based on the observed behavior, we named the switch on the right-hand side the ‘LFO switch’ and the one on the left the ‘feedback switch’. Both switches have two modes (‘on’ and ‘off’) so overall there are four working modes.

The pedal was measured at different LFO speed settings for all switch combinations. Seven steps were used: 0%, 17%, 34%, 50%, 67%, 84%, and 100% of the speed range. These steps were chosen because the knob of the speed potentiometer was seven-

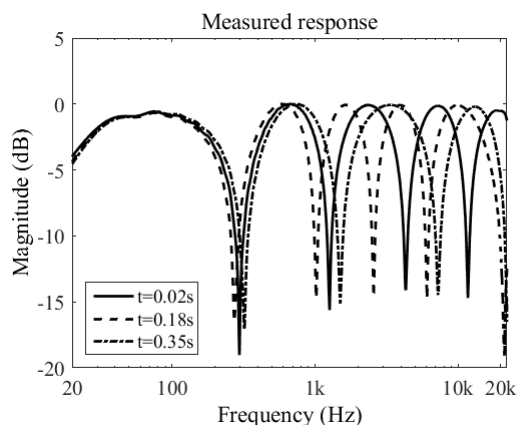


Figure 9: Magnitude response of the measured pedal at different times.

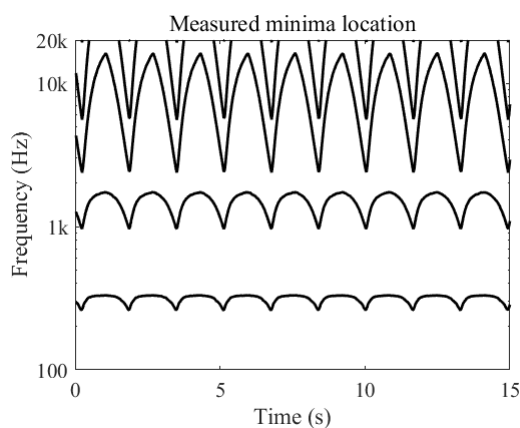


Figure 10: Estimated notches of the phaser pedal over time (LFO speed at approx. 50%, LFO and feedback switches both ‘off’).

sided and the pedal did not have any marks printed on it. Then the angles of the knob made it easy to see when the speed had increased by $1/7^{\text{th}}$ of its range. All measurements were conducted at a 48-kHz sampling rate.

4.1. Measurements with both switches OFF

The Fame pedal was measured with both switches in the ‘off’ position using a 25-s test signal synthesized using non-overlapping chirps placed at 30 ms intervals. Fig. 9 shows the measured magnitude response at three different times. In this figure, we can observe that the pedal introduces five notches, with the fifth one lying well above 20 kHz. This means the phaser most likely operates around a 10-stage filter network, another indication that the studied pedal is a clone of the MXR Phase 100.

Fig. 10 shows the estimated notch trajectories during a 15-second period. These data were generated using the method described in the previous section. This figure reveals the existence of five notches, with the fifth one lying mostly outside the audible range. It can also be noticed that the first notch has a range of about a quarter of an octave, the second one has roughly one octave, and the third one has about three octaves. Additionally, the

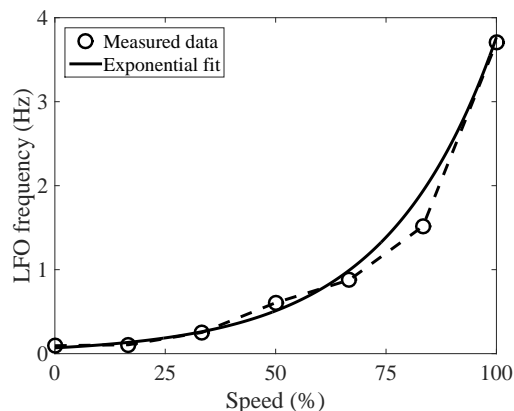


Figure 11: Measured LFO frequency with seven different speed settings and an exponential fit.

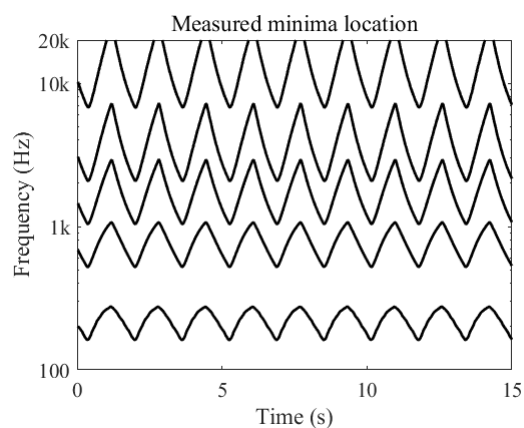


Figure 12: Estimated notches of the measured phaser over time with the LFO switch ‘on’ and speed at approx. 50%.

notch trajectories seem to resemble a full-wave rectified sinewave. This suggests that the LFO has this waveform in the ‘off’ mode, rather than the typical triangular or sinusoidal shapes.

Moving on with the measurements, Fig. 11 shows the effect of the speed potentiometer, which is approximately exponential. The LFO range can be observed to be from about 0.1 Hz to 3.7 Hz. These frequencies were estimated from the time differences between the lowest notch locations. For instance, in Fig. 10 the time difference between the lowest notch locations is approx. 1.6 s, which corresponds to the LFO frequency of about 0.6 Hz.

4.2. Effect of the LFO switch

The pedal was measured again with the LFO switch in the ‘on’ position. The overall appearance of the resulting magnitude responses were observed to be similar to the case of both switches turned ‘off’. The LFO speed measurements also remained unchanged. The main observed difference was the behavior of the notches over time. This can be seen in Fig. 12, where it can be noticed that the notch trajectories resemble triangular waves now. Secondly, all five notches are now visible in the spectrum. In the previous measurements only three notches were within the audible band during an entire cycle; the fourth notch was only partially

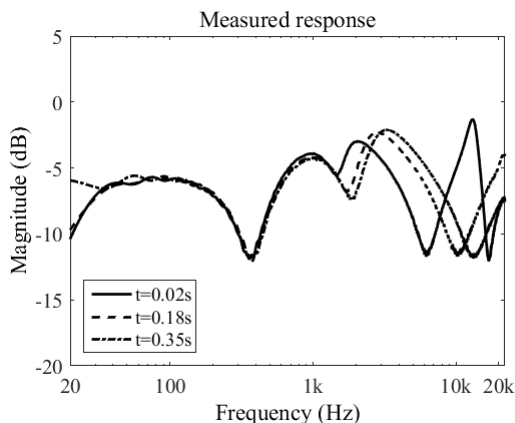


Figure 13: Magnitude responses of the measured phaser at different times with the feedback switch in the ‘on’ position (LFO speed 50%).

visible and the fifth notch was above 20 kHz throughout the measurements. Therefore, it can be deduced that the right switch of the pedal modifies the waveshape and range of the LFO, causing the effect to be perceived as more ‘intense’, hence the label on the pedal’s enclosure.

4.3. Effect of the feedback switch

From the measurements of the pedal with the feedback switch ‘on’ it was observed that the minima and speed behavior remained identical to the ‘off’ case. However, differences were observed in the magnitude response of the pedal. These changes are quite drastic, as the gain between the notches is boosted, the notch depths vary considerably with time, and the overall shape of the magnitude responses at any given time is considerably different. This behavior is shown in Fig. 13. It can be assumed that the left switch activates a feedback path to the allpass filter chain, as the changes in the response are similar to those seen in Fig. 4.

As a final note on the measured data, when both switches were in the ‘on’ position, the resulting responses were a combination of both effects: The notch behavior was similar to that of Fig. 12, and the magnitude response behaved as in Fig. 13.

5. MODELING OF THE MEASURED PHASER

A gray-box digital model of the measured phaser was implemented based on the collected data. Several design choices were made based on basic knowledge of the internal workings of phaser pedals, hence the term gray-box. First, it was decided to use first-order allpass filters only, as these are the building blocks of standard analog phaser pedals [2, 9]. This design makes it impossible to control the width of the notches independently, but is faithful to the original analog design. Since measurements showed that the phaser introduces five notches, the designed called for a network of ten first-order allpass filters paired in groups of two. Then, with the help of a simplified study of the circuit [13], it was observed that the first and last pairs of filters were not being modulated. This can be written as

$$A_1 = A_2 = A_9 = A_{10} \quad (5)$$

$$A_3 = A_4 = A_5 = A_6 = A_7 = A_8 \quad (6)$$

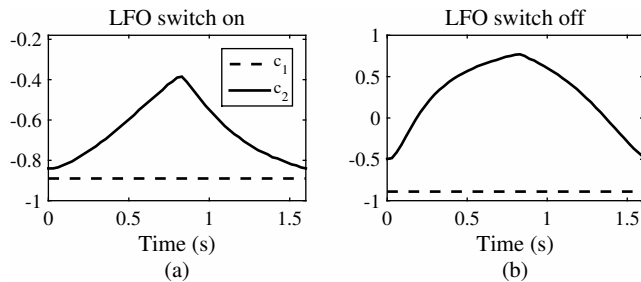


Figure 14: Estimated values of allpass filter coefficients c_1 and c_2 for a single LFO cycle, when the LFO switch is (a) ‘on’ and (b) ‘off’.

where A_m is the transfer function of the m^{th} allpass filter. This means that only two coefficients are needed to model the phaser.

The location of the notches over a single LFO cycle for both positions of the LFO switch were readily available from the measurements shown in Figs. 10 and 12. An algorithm was devised to find the pair of coefficients that best fit the measured data. This was done by iterating over a large set of coefficient combinations and evaluating the phase response of the allpass network at the target frequencies analytically and computing the mean absolute error. This optimization was performed using a standard sampling rate of 44.1 kHz.

After some initial tests, it was observed that the pair of coefficients that gave the smallest error performed rather poorly at low frequencies. This was attributed to the inaccurate nature of analog systems. Even when the filters used in the original analog pedal are supposed to be identical, the high tolerance levels of the components make this condition impossible. To minimize this effect, we decided to neglect the fourth and fifth notches for the case of the LFO switch ‘off’ and the fifth notch for the case of the LFO switch ‘on’ during the optimization process.

Several coefficient evaluations demonstrated the initial assumption that the first and last pair of allpass filters are static. Based on testing, coefficient c_1 , i.e. the coefficient for filters A_1, A_2, A_9 , and A_{10} was assigned a fixed value of -0.89 . Fig. 14(a) shows the estimated value for coefficient c_2 , i.e. the coefficient for filters $A_3 \dots A_8$, for a single cycle when the LFO switch is ‘on’. As inferred from the measurements, this coefficient can be modulated using a triangular LFO. The range of this LFO must be between $[-0.84, -0.39]$. Fig. 14(b) shows the estimated values for c_2 when the LFO switch is in the ‘off’ position. This LFO can be modeled using a rectified sine wave ranging between $[-0.49, 0.77]$.

The LFO speed control was modeled with a weighted least squares fit of an exponential function to the data shown in Fig. 11:

$$f_{lfo} = 0.069e^{0.040s}, \quad (7)$$

where $0 \leq s \leq 100$ is the LFO speed parameter and f_{lfo} is the fundamental frequency of the LFO.

To validate the model, a test signal was phasered with the model using coefficients estimated previously. A second-order IIR filter was used to simulate the DC blocker observed in the measurements. A DC blocking filter is common in analog audio electronics and is used to remove hum [14] or to assure that the waveform is symmetric before it enters a distortion unit. The transfer function

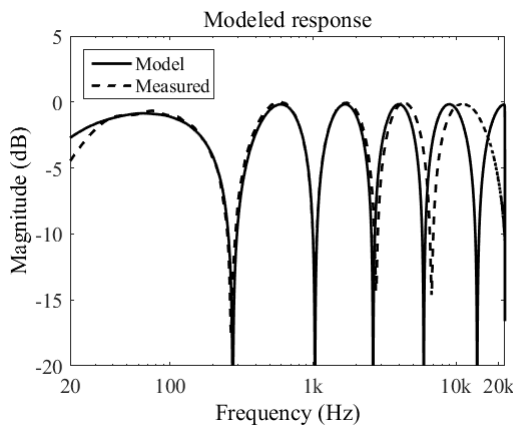


Figure 15: Magnitude response of the modeled phaser compared to the measured response with the LFO switch ‘off’. Parameters $G = 0.5$ and $W = 0.5$ were used.

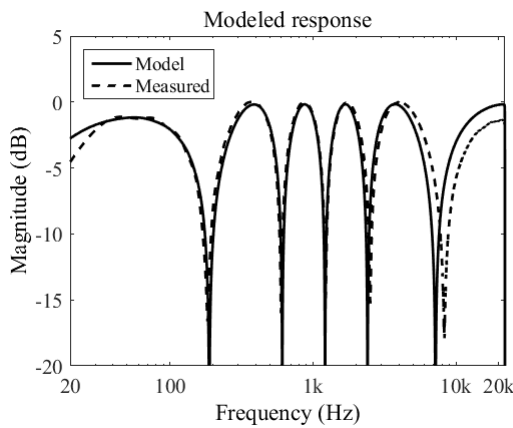


Figure 16: Magnitude response of the modeled phaser compared to the measured response with the LFO switch ‘on’ ($G = W = 0.5$).

of the second-order DC blocker is

$$H_{DC} = \frac{1+p}{2} \frac{1-z^{-2}}{1-pz^{-2}}, \quad (8)$$

where $p = 0.992$ determines the pole location, which is an octave lower than in the corresponding first-order design [14].

The phasered test signal was then analyzed using the same method as the pedal measurements, and the magnitude responses and notch frequencies at each time were found. A comparison of the model’s magnitude response to that of the measured pedal in Fig. 15 and Fig. 16 shows a close resemblance, but it can also be seen that the notch frequencies are matched much better at low than at high frequencies. Perceptually, the model accuracy in the highest octave is not highly important, however.

When comparing the behavior of notches in the model, shown in Fig. 17 and Fig. 18, and in the measured pedal (see Fig. 10 and Fig. 12), it can be noticed that they are very similar. The measured and the modeled notches have nearly the same the period, waveform, and frequency range. This can easily be seen in Fig. 19 in which the notches of both the measured and the modeled phaser are synchronized in time and are plotted for roughly two periods

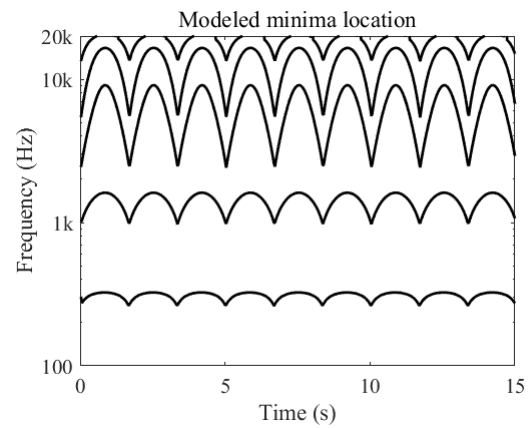


Figure 17: Estimated notch frequencies of the digital phaser model emulating the case when the LFO switch is ‘off’ (full-wave rectified sine LFO), the feedback switch is ‘off’, and the speed is set at 54%. Cf. Fig. 10.

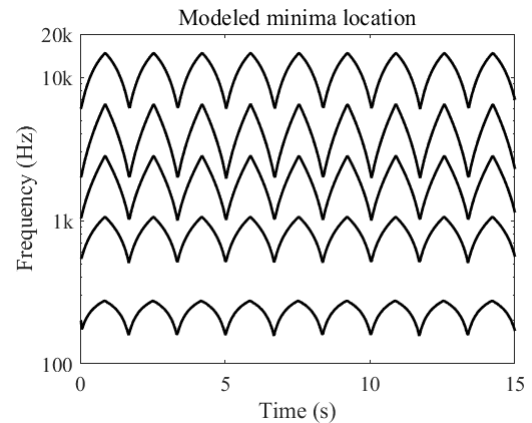


Figure 18: Estimated notch frequencies of the digital phaser model emulating the case when the LFO switch is ‘on’ (triangular LFO), the feedback switch is ‘off’, and the speed is set at 54%. Cf. Fig. 12.

with zoomed in frequency axis to better see the differences. One reason for the minor deviation is the LFO waveshape, which was modeled as strictly triangular in this case. However, an analog LFO of a phaser does not produce a perfect triangular waveform, but there is some degree of curvature in the waveform.

Furthermore, modeling of the phaser with the feedback was tested, but it was noticed that the model used could not produce a response identical to the measured one with the feedback switch ‘on’. An example of the model’s response with feedback is shown in Fig. 4. It can be compared to the response of the measured system in Fig. 13. In the model, the notch locations are again correct, but the resonances between the notches cannot be matched with those of the measured system.

Sound examples and Matlab code related to this work are available online [15].

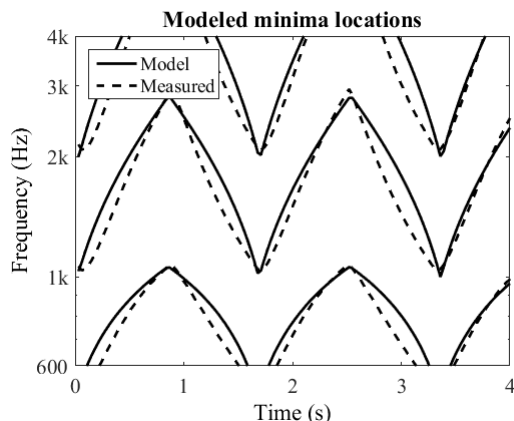


Figure 19: Comparison of three notches of the measured and modeled phaser as a function of time (LFO switch ‘on’; triangular LFO).

6. CONCLUSIONS

A method to measure time-varying audio effects was proposed. It uses a sequence of very short chirps to measure the impulse response of the system under measurement multiple times, and from them a characterization of the system can be produced. In the case of phasers, the spectral notches at different times are extracted from the measurements. The behavior of the magnitude response and notch locations in time reveals the operating principle of the measured phaser.

The method was tested by measuring a phaser pedal, and the results were analyzed. For example, the LFO frequency for different speed settings was measured and an exponential mapping was observed. The effect of the two switches of the pedal were analyzed based on the measurements, with one changing the LFO signal’s waveshape and range while the other adding a feedback around the allpass filter loop. A gray-box virtual analog model of the phaser was calibrated based on the measurements.

In the gray-box model the idea was to emulate the measurements, making it easier through some knowledge of the pedal. Overall the resulting model behaved similarly as the data after which it was modeled. However, the modeling of the feedback feature was not accurate in details. It could be improved in the future by using a modeling technique which does not need a fictitious unit delay in the feedback loop [16, 17].

7. ACKNOWLEDGMENT

The helpful comments of anonymous reviewers are gratefully acknowledged.

8. REFERENCES

[1] J. Pakarinen and D. T. Yeh, “A review of digital techniques for modeling vacuum-tube guitar amplifiers,” *Computer Music J.*, vol. 33, no. 2, pp. 85–100, 2009.

[2] F. Eichas, M. Fink, M. Holters, and U. Zölzer, “Physical modeling of the MXR Phase 90 guitar effect pedal,” in *Proc. 17th Int. Conf. Digital Audio Effects (DAFx-14)*, Erlangen, Germany, 2014, pp. 153–158.

[3] U. Zölzer, *DAFX: Digital Audio Effects, 2nd Edition*, 2011.

[4] F. Eichas, M. Fink, and U. Zölzer, “Feature design for the classification of audio effect units by input/output measurements,” in *Proc. 18th Int. Conf. Digital Audio Effects (DAFx-15)*, Trondheim, Norway, Nov.–Dec. 2015, pp. 27–33.

[5] V. Välimäki, J. S. Abel, and J. O. Smith, “Spectral delay filters,” *J. Audio Eng. Soc.*, vol. 57, no. 7/8, pp. 521–531, Jul.–Aug. 2009.

[6] W. M. Hartmann, “Flanging and phasers,” *J. Audio Eng. Soc.*, vol. 26, no. 6, pp. 439–443, June 1978.

[7] M. L. Beigel, “A digital ‘phase shifter’ for musical applications, using the Bell Labs (Alles-Fischer) digital filter module,” *J. Audio Eng. Soc.*, vol. 27, no. 9, pp. 673–676, Sept. 1979.

[8] A. Huovilainen, “Enhanced digital models for analog modulation effects,” in *Proc. 8th Int. Conf. Digital Audio Effects (DAFx-05)*, Madrid, Spain, Sept. 2005, pp. 155–160.

[9] J. O. Smith, “An allpass approach to digital phasing and flanging,” in *Proc. Int. Comp. Music Conf.*, Paris, France, Oct. 1984, pp. 103–109.

[10] F. Esqueda, V. Välimäki, and J. Parker, “Barberpole phasing and flanging illusions,” in *Proc. 18th Int. Conf. Digital Audio Effects (DAFx-15)*, Trondheim, Norway, Nov.–Dec. 2015, pp. 87–94.

[11] S. Arnardottir, J. S. Abel, and J. O. Smith III, “A digital model of the Echoplex tape delay,” in *Proc. Audio Eng. Soc. 125th Conv.*, San Francisco, CA, Oct. 2008.

[12] D. Griesinger, “Impulse response measurements using allpass deconvolution,” in *Proc. Audio Eng. Soc. 11th Int. Conf. Test & Measurement*, Portland, OR, May 1992.

[13] J. D. Sleep, “MXR Phase 100 Phase Shifter [Online],” http://www.generalguitargadgets.com/pdf/ggg_p100_sc.pdf, 2009, Accessed 9 June 2016.

[14] J. Pekonen and V. Välimäki, “Filter-based alias reduction for digital classical waveform synthesis,” in *Proc. IEEE Int. Conf. Acoust. Speech Signal Process. (ICASSP)*, Las Vegas, NV, Mar.–Apr. 2008, pp. 133–136.

[15] R. Kiiski, F. Esqueda, and V. Välimäki, “Supplementary materials for time-variant gray-box modeling of a phaser pedal [Online],” <http://research.spa.aalto.fi/publications/papers/dafx16-phaser/>, 2016, Accessed 10 June 2016.

[16] F. Fontana, F. Avanzini, and D. Rocchesso, “Computation of nonlinear filter networks containing delay-free paths,” in *Proc. Int. Conf. Digital Audio Effects (DAFx-04)*, Naples, Italy, Oct. 2004, pp. 113–118.

[17] D. Medine, “Dynamical systems for audio synthesis: Embracing nonlinearities and delay-free loops,” *Applied Sciences*, vol. 6, no. 5/134, 10 May 2016, Available online at <http://www.mdpi.com/2076-3417/6/5/134>.